

# Analysis of vibration attenuation characteristics of large thickness carbon fiber composite laminates

Yi-Qi WANG\*, Chaoqun WANG, Pengxiao YANG, Ziao WANG, Tete CAO

Key Laboratory for Precision and Non-traditional Machining Technology of Ministry of Education, Dalian University of Technology, Dalian 116024, China

\*Corresponding Author: Yi-Qi WANG, E-mail address: wangyiqi@dlut.edu.cn

## Abstract:

The vibration attenuation and damping characteristics of carbon fiber reinforced composite laminates with different thicknesses were investigated by hammering experiments under free boundary constraints in different directions. The dynamic signal testing and analysis system is applied to collect and analyze the vibration signals of the composite specimens, and combine the self-spectrum analysis and logarithmic decay method to identify the fundamental frequencies of different specimens and calculate the damping ratios of different directions of the specimens. The results showed that the overall stiffness of the specimen increased with the increase of the specimen thickness, and when the thickness of the sample increases from 24mm to 32mm, the fundamental frequency increases by 35.1%, the vibration showed the same vibration attenuation and energy dissipation characteristics in the 0° and 90° directions of the specimen, compared with the specimen in the 45° direction, which was less likely to be excited and had poorer vibration attenuation ability, while the upper and lower surfaces of the same specimen showed slightly different attenuation characteristics to the vibration, the maximum difference of damping capacity between top and bottom surfaces of CFRP plates is about 70%.

**Keywords:** Carbon fiber composite laminates; Logarithmic decay method; Damping ratio; Natural frequency

## Introduction

Carbon fiber reinforced polymer (CFRP) have been widely used in aerospace, automotive and defense industries [3-6] due to their high specific strength and specific stiffness [1-2]. Due to the unique weight reduction advantages of carbon fiber composites, the application of large thickness CFRP is also becoming more and more common, such as a series of Airbus aircraft with large thickness CFRP joints and central wing boxes. In addition to meeting various mechanical properties, the vibration damping properties of CFRP are also very important, which affect the performance, safety and reliability of parts and systems [7]. As the most widely used marine propulsion device, the noise and vibration generated by ship propeller cannot be ignored. At present, there have been a lot of research on composite propellers to eliminate violent vibration [8-9].

Damping can be defined as the energy dissipation of a structure that generates vibrations [10-12]. The damping mechanism attenuates the vibration by converting the energy generated by the vibration into other forms of energy. While CFRP belongs to fiber reinforced resin

matrix composites, its damping properties are significantly anisotropic as well as mechanical properties.

Gibson [13] and Zou [14] have made great contributions to the analysis of vibration testing methods by investigating modal testing techniques, including frequency response methods and time domain analysis as well as frequency domain analysis, to further analyze and study the response of structures subjected to excitation. In terms of experimental tests, Adams [15-16] and others used free beam bending vibration experiments to study the dynamic properties and damping of unidirectional composites at different temperatures. Pei and Li [17] used hammering experimental methods to study the effect of fiber orientation on the modal and damping ratios of unidirectional carbon fiber composite laminates. Riccardo [18] investigated the modal damping parameters of composite laminates by an experimental method of point-by-point excitation single-point test. Rueppel [19] and others applied logarithmic decay method and DMA analysis to analyze and study the damping properties of CFRP laminates and obtained the relationship between lay-up angle and damping properties. Pereira [20-21] used a combination of numerical calculations and experiments to preliminarily verify that variable angle lay-up can one

adjust the laminate frequency and damping, and further investigated the multi-objective optimization to improve the fundamental modal frequency and the corresponding specific damping capacity of the laminate. In the study of the damping energy dissipation mechanism of CFRP, Tang [22] reviewed the damping mechanism of fiber-reinforced resin matrix composites. It can be seen that the research on CFRP materials is mainly focused on the overall damping characteristics in depth, while the research on the attenuation law and damping characteristics of vibration in different directions within CFRP laminates is very little at present.

This paper focuses on the damping characteristics in different directions on a large thickness CFRP laminate. Hammering experiments are used to analyze the attenuation of vibrations within large thickness CFRP laminates (the thickness is greater than 3mm) of different thicknesses in different directions on the upper and lower surfaces by means of frequency and time domains.

## 1 Experimental preparation

### 1.1 CFRP Specimen preparation

Two specimens were prepared by Resin transfer molding (RTM) process using T300 grade  $0^\circ/90^\circ$  plain weave carbon fiber woven fabric. And E-51 resin is selected, which is produced by Wuxi Qianguang Chemical Materials Co. LTD. Different layers of the woven fabric were applied and the final CFRP specimens with thicknesses of 24 mm and 32 mm were obtained.

### 1.2 Experimental methods and apparatus

The hammer pulse method is based on frequency response functions and is widely used to describe the dynamic properties of vibrating systems [23].

The vibration test system is shown in Figure 1. The specimen is suspended on the experimental stand by a rubber elastic rope with certain stiffness to ensure free boundary conditions. The acceleration sensor is fixed at the measurement point with 502 binder and the output signal is sent to the data acquisition analyzer (INV3062-C1), and then the response signal is analyzed by the Coinv DASP V11 software.

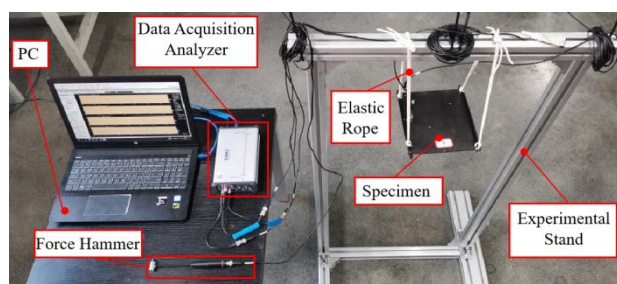


**Figure 1** The vibration test system for CFRP laminate

The vibration sensor measurement point arrangement diagram is shown in Figure 2. The CFRP specimen was struck using an INV9310 impact force hammer to make the specimen vibrate freely and return to rest with damping, and six sets of experiments were conducted in six directions. Each experiment sensor was arranged at the center and end points of one of the  $0^\circ$ ,  $45^\circ$  and  $90^\circ$  directions on the top surface (TS) and bottom surface (BS), respectively. Three taps were performed for each set of experiments, and the data were averaged to ensure the accuracy of the analysis.

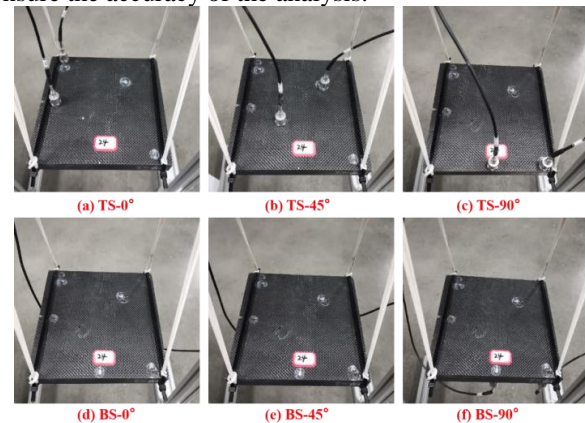


**Figure 2** Arrangement of measurement points of acceleration sensors in different directions

(a) TS- $0^\circ$  (b) TS- $45^\circ$  (c) TS- $90^\circ$  (d) BS- $0^\circ$   
(e) BS- $45^\circ$  (f) BS- $90^\circ$

## 2 Results and discussion

### 2.1 Analysis of inherent frequency

The magnitude of the first natural frequency (i.e. fundamental frequency) of the laminate is a key indicator of the vibration characteristics of the structure. The acceleration output signal collected by the collector is processed by the software as a spectrogram, and the spectrogram is used to identify the first-order intrinsic frequency. The spectrum analysis of the collected data was carried out by Fast Fourier Transform (FFT).

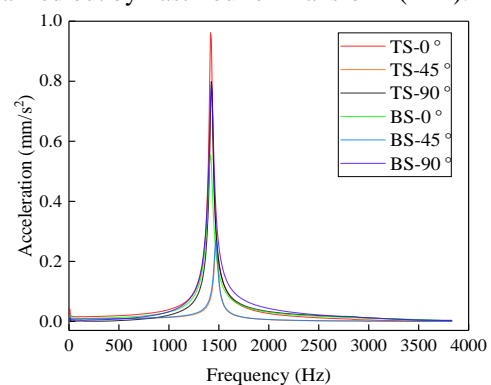


**Figure 3** Spectra of the end points of the specimen with thickness of 24mm in each direction

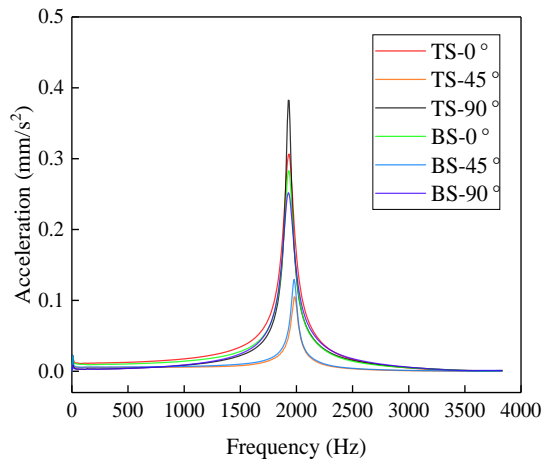


**Figure 4** Spectra of the end points of the specimen with thickness of 32mm in each direction

The comparative analysis of Figure 3 and Figure 4 shows that the two specimens exhibit the same vibration law in the 0° and 90° directions on the upper and lower surfaces, and the same intrinsic frequencies can be calculated in these four directions. While in the 45° direction of the upper and lower surfaces showed a slight difference. Through the self-spectrum analysis of the specimen in 0° and 90° directions, it can be seen that the first-order inherent frequencies of the specimens with thicknesses of 24 mm and 32 mm are 1425.0 Hz and 1925.7 Hz, respectively. With the increase of the specimen thickness, the fundamental frequency of the specimen increases, which is closely related to the overall stiffness of the plate, and the specimens with better stiffness are less likely to resonate. While, the 45° directional curves of the two specimens with thicknesses of 24 mm and 32 mm calculated a slight increase in the intrinsic frequency with a boost of 3.16% and 2.59%. This shows that the transmission of vibration in the 45° direction is different from the 0° and 90° directions. Since the experimentally used CFRP is an anisotropic material with different strength and stiffness in either internal direction other than the fiber direction, and the stiffness in the 45° direction is increased relative to the fiber direction, the slightly higher fundamental frequency analysis results are identified and calculated.

## 2.2 Analysis of Logarithmic decrement

In the time domain waveform analysis, as shown in Figure 5 and Figure 6, the acceleration waveforms at the end points in each direction decay exponentially. Therefore, the free vibration decay method is the most intuitive and simple method to represent the vibration decay and damping performance of the end points in each direction.

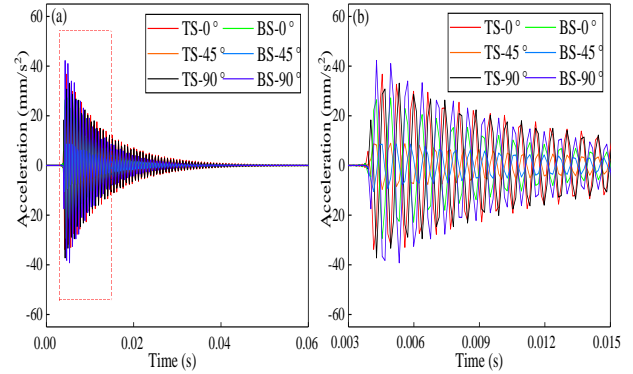


**Figure 5** Time domain waveforms at the end points in each direction for a 24 mm thick specimen: (a) Full time domain diagram, (b) Time domain diagram of the start-up phase

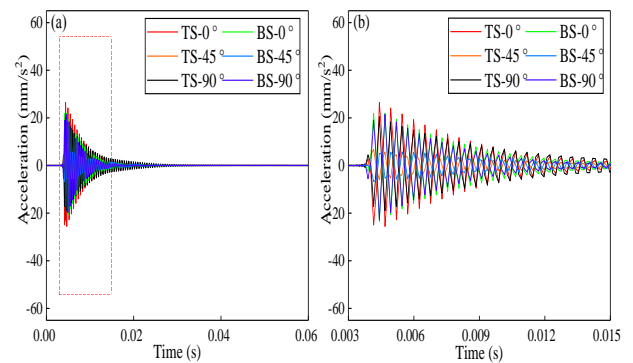


**Figure 6** Time domain waveforms at the end points in each direction for a 32 mm thick specimen: (a) Full time domain diagram, (b) Time domain diagram of the start-up phase

Logarithmic decrement ( $\delta$ ) is commonly used as a parameter to characterize the damping properties of a material and is calculated as

$$\delta = \frac{1}{m} \ln \frac{A_n}{A_{n+m}} \quad (1)$$

where  $A_n$  and  $A_{n+m}$  are the  $n$ th and  $(n+m)$  th amplitudes on the decay curve, respectively.

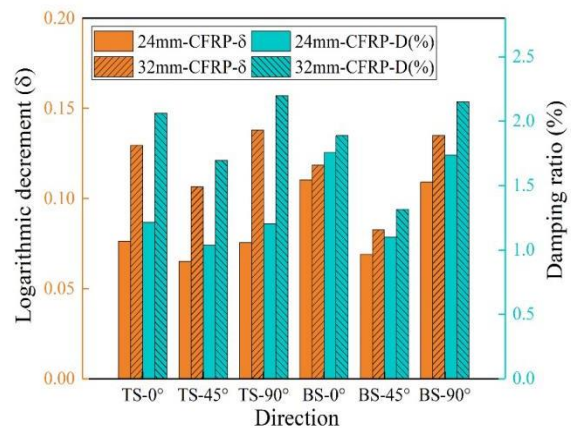


**Figure 7** Logarithmic decrement and damping ratio of each direction of the two specimens

As can be seen in Figure 7, the specimen with a thickness of 32 mm has a higher logarithmic attenuation rate than the 24 mm specimen in all six directions measured, i.e., the 32 mm thickness specimen has a better attenuation effect on the vibration in these directions. In addition, when combined with Figure 5 and Figure 6, the two specimens were subjected to the same excitation force to generate vibration, the 32 mm CFRP plate recovered its initial stationary state in a shorter time. Moreover, combined with the time-domain waveforms, it can also be seen that the 45° direction has significantly lower vibration acceleration amplitude than the 0° and 90° directions at the onset of vibration. The reason for this is that CFRP has higher stiffness in the non-fiber direction of 45°, and has lower sensitivity and higher stability to shock and vibration. 32mm specimens show less susceptibility to excitation and more rapid abatement.

There are certain patterns and differences in the logarithmic attenuation rates in different directions of the same specimen. Compared with the 45° direction on both surfaces, the vibration attenuation ability is better in the 0° and 90° directions. 24mm specimens have better vibration attenuation ability in the 45° direction on the lower surface, while 32mm shows the opposite pattern.

### 2.3 Analysis of damping ratio

The damping ratio makes a dimensionless measure relative to the amplitude decay rate and represents the form of decay of the vibration of the specimen after being excited. The relationship between the logarithmic decay rate and the damping ratio is shown in Equation 2.

$$\delta = \frac{2\pi\zeta}{\sqrt{1-\zeta^2}} \approx 2\pi\zeta \quad (2)$$

Therefore, the damping ratio of each direction of the specimen can be calculated by Equation 3. The calculation results are also shown in Figure 7.

$$\zeta = \frac{\delta}{2\pi} \quad (3)$$

The trend of the damping ratio in each direction of the two specimens in Figure 7 shows that the 32mm CFRP specimen has better damping performance than the 24mm specimen, and this characteristic is especially shown in the specimen for vibration transmission in the in-plane. For example, the damping ratio in the 0° direction on the upper and lower surfaces is 69.78% higher than that of the 24 mm specimen, while the damping ratio in the 0° direction on the lower surface is only 7.40% higher than that of the 24 mm specimen.

For the same specimen, the vibration dissipation ability is very similar in the 0° and 90° directions, both directions are fiber directions, and the stiffness is the same in the in-plane. And the damping is lower than in the 45° direction for the upper and lower surfaces, which indicates that the vibration dissipation ability is relatively poorer in that direction. For the upper and lower surfaces, in the 0° and 90° directions, the energy dissipation

ability of the lower surface is slightly higher or close to the same direction of the upper surface, which indicates that the damping performance of the thickness direction also plays a certain role when the vibration is transmitted to the lower surface under the same hammering force knocking situation, but its role is very limited, while in the 45° direction, the damping ability of the upper and lower surfaces is not much different.

## 3 Conclusion

Single-point impulse hammering experiments were conducted on two CFRP specimens with different thicknesses. The time domain analysis and the self-spectral analysis curves calculated by FFT were obtained by arranging acceleration sensors at the center and end points of 0°, 45° and 90° directions on the upper and lower surfaces of the specimens to study the attenuation and damping characteristics of the vibration in different directions on the two surfaces.

(1) The increase in thickness increases the overall stiffness of the CFRP laminate. The specimen with a thickness of 32 mm has a significant increase in the first natural frequency compared to the specimen with a thickness of 24 mm, and is also less likely to be excited.

(2) The results of the intrinsic frequencies of the specimens obtained by the self-spectral analysis curves differ in the 45° direction and other directions, and the calculated results in the 45° direction are slightly higher. Combined with the maximum amplitude of the end-point vibration in each direction on the time domain analysis curve, the 45° direction also shows a lower level. Both confirm that the CFRP plate has higher stiffness and insensitivity and stability to vibration and impact in the 45° direction on the upper and lower surfaces of the CFRP laminate.

(3) By comparing the results of logarithmic decrement and damping ratio at the end points of different directions, it can be found that the logarithmic decrement and damping ratio in the 45° direction are significantly lower than those in the other directions, which also indicates that this direction has higher stiffness and thus leads to worse damping performance in this direction, for the 0° and 90° directions (fiber direction) of the top and bottom surfaces of the specimen, the damping performance shows consistency.

## Acknowledgments

This work was supported by the Fundamental Research Funds for the Central Universities [grant nos. DUT21LAB108, DUT22LAB401].

## References

- [1] Werken N, Tekinalp H, Khanbolouki P, et al, 2019. Additively Manufactured Carbon Fiber-Reinforced Composites: State

- of the Art and Perspective. *Additive Manufacturing*, (31): 100962.
- [2] Du X, Zhou H, Sun W, et al, 2017. Graphene/epoxy interleaves for delamination toughening and monitoring of crack damage in carbon fibre/epoxy composite laminates. *Composites Science and Technology*, (140): 123-133.
- [3] Venkatachari A, Natarajan S, Haboussi M, et al, 2016. Environmental effects on the free vibration of curvilinear fibre composite laminates with cutouts. *Composites Part B*, (88): 131-138.
- [4] Subramani M, Ramamoorthy M, 2020. Vibration analysis of multiwalled carbon nanotube-reinforced composite shell: An experimental study. *Polymers and Polymer Composites*, 28(4): 223-232.
- [5] Treviso A, Genechten BV, Mundo D, et al, 2015. Damping in composite materials: Properties and models. *Composites Part B: Engineering*, (78): 144-152.
- [6] Yan L, Sc A, Xh A, 2017. Multi-scaled enhancement of damping property for carbon fiber reinforced composites. *Composites Science and Technology*, (143):89-97.
- [7] Zhang J, Yang H, Chen G, 2019. Damping of carbon fibre-reinforced plastics plates with holes. *Plastics, Rubber and Composites*, 48(10): 432-439.
- [8] Mao Y, Young Y L, 2016. Influence of skew on the added mass and damping characteristics of marine propellers. *Ocean Engineering*, 121: 437-452.
- [9] Mulcahy N L, Prusty B G, Gardiner C P, 2010. Hydroelastic tailoring of flexible composite propellers. *Ships and Offshore structures*, 5(4): 359-370.
- [10] Abramovich H, Govich D, Grunwald A, 2015. Damping measurements of laminated composite materials and aluminum using the hysteresis loop method. *Progress in Aerospace Sciences*, (78): 8-18.
- [11] Assarar M, Zouari W, Ayad R, et al, 2018. Improving the damping properties of carbon fibre reinforced composites by interleaving flax and viscoelastic layers. *Composites Part B: Engineering*, (152): 248-255.
- [12] Lin H, Xiang Y, Yang Y, 2016. Coupled vibration analysis of CFRP cable-tube system under parametric excitation in submerged floating tunnel. *Procedia engineering*, (166): 45-52.
- [13] Gibson R F, 2000. Modal vibration response measurements for characterization of composite materials and structures. *Composites Science and Technology*, 60(15): 2769-2780.
- [14] Zou Y, Tong L, Steven G P, 2000. Vibration-based model-dependent damage (delamination) identification and health monitoring for composite structures - a review. *Journal of Sound and vibration*, 230(2): 357-378.
- [15] Adams R D, Maheri M R, 2003. Damping in advanced polymer-matrix composites. *Journal of Alloys & Compounds*, 355(1-2): 126-130.
- [16] Maheri M R, Adams R D, 2003. Modal vibration damping of anisotropic FRP laminates using the Rayleigh – Ritz energy minimization scheme. *Journal of sound and vibration*, 259(1): 17-29.
- [17] Pei X Y, Li J L, 2012. The effects of fiber orientation on the vibration modal behavior of carbon fiber plain woven fabric/epoxy resin composites. *Advanced Materials Research*. Trans Tech Publications Ltd, 391: 345-348.
- [18] Vescovini R, Bisagni C, 2015. A procedure for the evaluation of damping effects in composite laminated structures. *Progress in Aerospace Sciences*, 78: 19-29.
- [19] Rueppel M, Rion J, Dransfeld C, et al, 2017. Damping of carbon fibre and flax fibre angle-ply composite laminates. *Composites Science & Technology*, 146: 1-9.
- [20] Pereira D A, Guimarães TAM, Resende H B, et al, 2020. Numerical and experimental analyses of modal frequency and damping in tow-steered CFRP laminates. *Composite Structures*, 244: 112190.
- [21] Pereira D A, Sales T P, Rade D A, 2021. Multi-objective frequency and damping optimization of tow-steered composite laminates. *Composite Structures*, 256: 112932.
- [22] Tang X, Yan X, 2020. A review on the damping properties of fiber reinforced polymer composites. *Journal of Industrial Textiles*, 49(6): 693-721.
- [23] Ding G, Xie C, Zhang J, et al, 2016. Modal analysis based on finite element method and experimental validation on carbon fibre composite drive shaft considering steel joints. *Materials Research Innovations*, 19(sup5): 748-753.